Coherent control of the formation of cold heteronuclear molecules by photoassociation

Emanuel F. de Lima*

Departamento de Física, Universidade Federal de São Carlos, São Carlos, SP 13565-905, Brazil

(Received 10 October 2016; revised manuscript received 14 December 2016; published 24 January 2017)

We consider the formation of cold diatomic molecules in the electronic ground state by photoassociation of atoms of dissimilar species. A combination of two transition pathways from the free colliding pair of atoms to a bound vibrational level of the electronic molecular ground state is envisioned. The first pathway consists of a pump-dump scheme with two time-delayed laser pulses in the near-infrared frequency domain. The pump pulse drives the transition to a bound vibrational level of an excited electronic state, while the dump pulse transfers the population to a bound vibrational level of the electronic ground state. The second pathway takes advantage of the existing permanent dipole moment and employs a single pulse in the far-infrared domain to drive the transition from the unbound atoms directly to a bound vibrational level in the electronic ground state. We show that this scheme offers the possibility to coherently control the photoassociation yield by manipulating the relative phase and timing of the pulses. The photoassociation mechanism is illustrated for the formation of cold LiCs molecules.

DOI: 10.1103/PhysRevA.95.013411

I. INTRODUCTION

The production of dense samples of cold and ultracold molecules is an important goal for physics and chemistry due to their potential applications, which range from the elaboration of quantum computing methodologies to the study of ultracold chemical reactions [1–4]. In particular, the creation of cold gases of polar molecules has been attracting considerable attention owing to the long-range dipole-dipole interaction of these systems [5–13]. A possible route to obtain such cold samples is to form molecules by photoassociation of cold atoms, where a colliding pair is bound together through the interaction with an external electromagnetic field [14–18]. This process is usually achieved by a laser-induced transition from the free atoms to an electronic excited state of the molecule. In order to obtain molecules in the electronic ground state, which is important for many proposals, the molecule is deexcited by either spontaneous or induced emission. In pump-dump photoassociation schemes, a sequence of two laser pulses is employed [19–22]. The pump pulse excites a wave packet in the electronically excited state, while the dump pulse transfers the wave packet back to the electronic ground state. One benefit of this approach is that, using the time delay between the pulses, the photoassociation yield can be controlled by quantum interference, which is in the heart of coherent control [23–27].

The existence of a permanent dipole moment in heteronuclear molecules offers yet another pathway for photoassociation: a free-to-bound electric-dipole transition can be induced by an external electromagnetic field within the electronic ground state [28–32]. Though restricted to heteronuclear molecules, this approach has the advantage of not depending on the structure and lifetime of electronic excited states. In contrast with the above-mentioned photoassociation mechanism, which involves visible or near-infrared radiation, this scheme relies on transitions in the microwave or far-infrared range.

The aim of the present work is to show that these two photoassociation pathways can be made to interfere in order to coherently control the photoassociation yield. The overall strategy involves three pulses, a pair of pump-dump pulses in the near-infrared frequency domain, which excites transitions involving an electronic excited state, along with a pulse in the far-infrared domain, involving transitions only in the electronic ground state. Calculations are performed within a model system for the photoassociation of ^{7}Li ^{133}Cs in the $X\,^1\Sigma$ ground state, which possesses a relatively large permanent dipole moment. We show that, through the manipulation of the relative timing and phases of the pulses, it is possible to control the formation of ground-state molecules.

II. TWO-PATHWAY SCHEME FOR PHOTOASSOCIATION

Consider the cold collision of two atoms of distinct species under the presence of external time-dependent electric fields. Assume the relative motion of the collision pair is initially taking place in the molecular electronic ground state. We contemplate two possible pathways leading to formation of a molecule in a bound vibrational level of the electronic ground state. Figure 1 schematically illustrates the photoassociation strategy for ^{7}Li + ^{133}Cs. In the first pathway, two laser pulses are employed in a pump-dump arrangement. The first pulse drives the transition from the initial state to a bound vibrational level ν' of an excited electronic state, while the dump pulse transfers the population to a vibrational bound level of the electronic ground state ν. In the second pathway, thanks to an associated dipole moment, a single external pulse induces a transition from the unbound initial state directly to the bound vibrational level ν within the ground electronic state.

We model the situation by means of the two-electronic-state Hamiltonian,

$$\hat{H}(t) = \begin{pmatrix} \hat{T}_g + \hat{V}_g - \hat{\mu}_g \cdot \varepsilon(t) & -\hat{\mu}_{ge} \cdot \varepsilon(t) \\ -\hat{\mu}_{ge} \cdot \varepsilon(t) & \hat{T}_e + \hat{V}_e - \hat{\mu}_e \cdot \varepsilon(t) \end{pmatrix}, \quad (1)$$

where $\hat{T}$ denotes the kinetic-energy operator, $\hat{V}$ the potential-energy operator, and $\hat{\mu}$ the dipole moment operator, with the subscript g referring to the electronic ground state and the

*eflima@ufscar.br

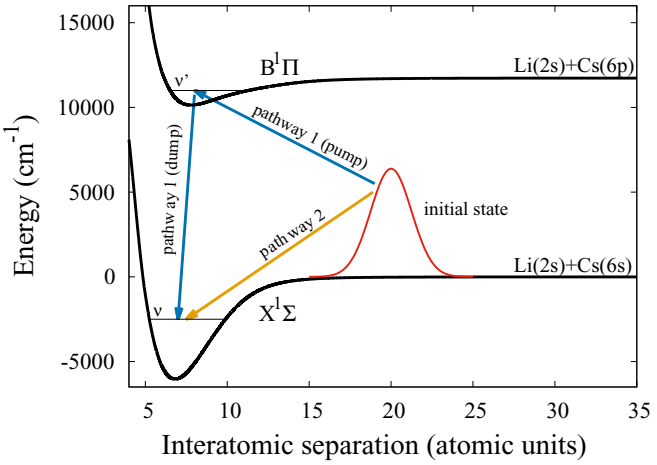

FIG. 1. Molecular potentials of LiCs along with a depiction of the photoassociation scheme (the initial state is not to scale). The pair of colliding atoms represented by the initial wave packet is transferred to a vibrational bound level of the electronic ground state through two different transition pathways.

subscript e to the excited state. $\hat{\mu}_{ge}$ is the transition dipole moment between the ground and excited electronic states. The external time-dependent electric field $\varepsilon(t)$ is composed of three pulses,

$$\varepsilon(t) = \sum_{i=1}^{3} S_i(t)\mathcal{V}_i \sin(\omega_i t + \phi_i) = \varepsilon_1(t) + \varepsilon_2(t) + \varepsilon_3(t), \tag{2}$$

with $S_i(t)$, $\mathcal{V}_i$, ω_i, ϕ_i, $i = 1,2,3$, being respectively the envelope functions, amplitudes, carrier frequencies, and phases of the pulses. The envelopes of the pulses are given by Gaussian functions,

$$S_i(t) = \exp\left[-2\ln 2\left(\frac{t - t_i'}{\tau_i}\right)^2\right], \tag{3}$$

where t_i' defines the temporal center and τ_i the full width at half maximum (FWHM) of each pulse. For definitiveness, $\varepsilon_1(t)$ refers to the pump pulse (pulse 1), $\varepsilon_2(t)$ refers to the dump pulse (pulse 2), and $\varepsilon_3(t)$ refers to the pulse corresponding to the second pathway (pulse 3).

We are interested in the solutions of the corresponding time-dependent Schrödinger equation,

$$i\hbar\frac{\partial}{\partial t}|\psi(t)\rangle = \hat{H}|\psi(t)\rangle, \tag{4}$$

for the two-component wave function,

$$\langle r|\psi(t)\rangle = \begin{pmatrix}\psi_g(r,t)\\ \psi_e(r,t)\end{pmatrix}, \tag{5}$$

where r is the interatomic distance. Here, we focus only in the vibrational motion, therefore neglecting the rotational motion. Apart from retaining the essential physics of the problem, this approximation is justified since our intention is to deal with low temperatures.

The energy spectrum of each molecular potential is composed of a set of discrete levels and a continuum region. As practical numerical solution of the dynamical equations often requires, we assume that the continuum part is suitably discretized, for instance, by the addition of an infinite barrier at long range, or equivalently, by the introduction of a spatial grid [33]. In the following, we label the discrete energy levels of the ground state by E_v with corresponding eigenfunctions $|\phi_v\rangle$ and the discretized continuum energy levels by E_n with corresponding eigenfunctions $|\phi_n\rangle$. The associated energy and eigenfunctions of the excited state are distinguished from those of the ground state by a prime symbol.

In order to disclose the control mechanism, we consider the transition from a discretized scattering level of the ground state, $|\phi_n\rangle$, to a target bound level of the ground state $|\phi_v\rangle$ through each photoassociation pathway separately. If the amplitude of the external field is sufficiently small, the final transition amplitude A_1 of the first pathway ($\varepsilon_3 = 0$) can be predicted by the second-order time-dependent perturbation theory [34],

$$A_1 = -\frac{1}{\hbar^2}\mu_{vv'}\mu_{v'n}\int_{-\infty}^{\infty} dt'\varepsilon(t')\exp(i\omega_{vv'}t') \times \int_{-\infty}^{t'} dt''\varepsilon(t'')\exp(i\omega_{v'n}t''), \tag{6}$$

where $\mu_{ij} \equiv \langle\phi_i|\hat{\mu}|\phi_j\rangle$ is the dipole moment and $\omega_{ij} \equiv (E_i - E_j)/\hbar$ is the Bohr frequency relative to the transition $j \to i$. In the above expression, we have assumed that only transitions involving the level v' of the excited state are within the spectral range of the external field. This formula can be written as [35]

$$A_1 = -\frac{1}{i\hbar^2}\mu_{vv'}\mu_{v'n}\left[i\pi\tilde{\varepsilon}(\omega_{vv'})\tilde{\varepsilon}(\omega_{v'n}) - P\int_{-\infty}^{\infty}\frac{\tilde{\varepsilon}(\omega)\tilde{\varepsilon}(\omega_{vn} - \omega)}{\omega - \omega_{v'n}}d\omega\right], \tag{7}$$

where $\tilde{\varepsilon}(\omega)$ is the Fourier transform of $\varepsilon(t)$ and P denotes the Cauchy principal value. The carrier frequencies of the first and second pulses, ω_1 and ω_2, are assumed to be very close to the resonance frequencies $\omega_{v'n}$ and $\omega_{v'v}$ of the transitions $|\phi_n\rangle \to |\phi_{v'}\rangle$ and $|\phi_{v'}\rangle \to |\phi_v\rangle$, respectively. We also assume that we are dealing with narrow-band pulses, meaning that the τ_1 and τ_2 are of the order of hundreds of picoseconds or larger, which correspond to frequency bandwidths of the order of 1 cm^{-1} or smaller. In the light of these considerations, we can retain only the resonant contributions and approximate the transition amplitude by

$$A_1 \approx -\frac{2\pi}{\hbar^2}\mu_{vv'}\mu_{v'n}\tilde{\varepsilon}_1(\omega_{v'n})\tilde{\varepsilon}_2(\omega_{vv'}). \tag{8}$$

Upon substituting the expressions for the field in Eq. (8), we obtain

$$A_1 \approx C_1\exp[i(\phi_2 - \phi_1)]\exp[i(\Delta_2 t_2 - \Delta_1 t_1)], \tag{9}$$

where $\Delta_1 = \omega_{v'n} - \omega_1$ and $\Delta_2 = \omega_{v'v} - \omega_2$ label the detuning from the resonances and

$$C_1 = -\frac{\pi}{\hbar^2}\mu_{vv'}\mu_{v'n}\sigma_1\sigma_2\mathcal{V}_1\mathcal{V}_2\exp[-(\sigma_1\Delta_1)^2 - (\sigma_2\Delta_2)^2], \tag{10}$$

with $\sigma_i = \tau_i/\sqrt{(8\ln 2)}$. Within the above approximations, the relative phase and timing of the pump and dump pulses have no impact on the transition probability taking the first pathway alone, as they imply in a global phase. Although that is not true in general for broadband, off-resonance fields, in which case nonresonant contributions need to be taken into account, this approximation suffices for the purposes of the present work, since we are interested in emphasizing the interference between the first and the second pathways.

The final transition amplitude A_2 of the second pathway ($\varepsilon_1 = 0$ and $\varepsilon_2 = 0$) can be predicted by the first-order time-dependent perturbation theory as being

$$A_2 = \frac{i}{\hbar}\mu_{vn}\int_{-\infty}^{\infty}\varepsilon(t')\exp(i\omega_{vn}t')dt' = \frac{i\sqrt{2\pi}}{\hbar}\mu_{vn}\tilde{\varepsilon}_3(\omega_{vn}). \tag{11}$$

Substituting $\varepsilon(t) = S_3(t)\mathcal{V}_3\sin(\omega_3 t + \phi_3)$ and assuming ω_3 is close to the resonance frequency ω_{nv} of the transition $|\phi_n\rangle \rightarrow |\phi_v\rangle$ we obtain

$$A_2 \approx C_2\exp\{i[\phi_3 + \Delta_3 t_3]\}, \tag{12}$$

where

$$C_2 = \frac{\sqrt{\pi}}{\hbar}\mu_{vn}\sigma_3\mathcal{V}_3\exp[-(\sigma_3\Delta_3)^2], \tag{13}$$

and $\Delta_3 = \omega_{vn} - \omega_3$. Again, no role is played by the phase or the timing of the third pulse if the second pathway is considered alone. However, the transition probability $P_{n\rightarrow v}$ from $|\phi_n\rangle$ to the target level $|\phi_v\rangle$ considering *both* pathways is given by

$$P_{n\rightarrow v} = |A_1 + A_2|^2 = C_1^2 + C_2^2 + 2\,\mathrm{Re}\{A_1 A_2^*\}, \tag{14}$$

where Re stands for the real part and

$$\mathrm{Re}\{A_1 A_2^*\} = C_1 C_2\cos[\Delta_2 t_2 - \Delta_1 t_1 - \Delta_3 t_3 + \phi_2 - \phi_1 - \phi_3]. \tag{15}$$

The above term represents the interference between the two transition pathways and it shows that the final transition probability can be controlled through manipulation of the timing and phases of the pulses. If we consider that the laser frequencies are set to the resonance transition frequencies $\Delta_i \approx 0$, the relative phases play a major role in controlling the transition probability from an initial stationary state.

We have performed calculations considering the $X\,^1\Sigma$ and $B\,^1\Pi$ states of LiCs as the ground and excited potentials $V_g(r)$ and $V_e(r)$, respectively. The potential-energy functions and dipole couplings were obtained from spline fittings based on data available in the literature [36–40]. In order to obtain the vibrational energies E_v and eigenfunctions $|\phi_v\rangle$ of each electronic state, we have resorted to the B-splines basis set with an exponential sequence of break points [41,42]. We have obtained 51 vibrational bound levels for the ground state and 34 bound levels for the excited state. In this approach, the continuum eigenfunctions are discretized in a large box of size $r_{\max}$ (we have used $r_{\max}$ typically of the order of 1500 atomic units). The number of discretized continuum levels was typically 800 for the ground state and 200 for the excited state.

Figure 2 shows the absolute value of the transition dipole moments $|\langle\phi_{v'}|\mu_{ge}|\phi_n\rangle|$ from the ground-state unbound level with energy $E_n = 0.035\ \mathrm{cm}^{-1} \approx 50$ mK to the bound levels v' of the excited state. Each full circle in the figure corresponds to a bound vibrational level. The horizontal axis corresponds to the energy gap between each bound level and the unbound level, which can also be thought of as the frequency of the pump pulse needed to make the corresponding transition. The maximum dipole moment is found for the $v' = 32$ level, corresponding to a transition energy of 11 731 cm^{-1}. Figure 3 shows the dipole moments between the ground and excited bound levels. Since the dipole $\mu_{ge}(r)$ function does not vary significantly over the range of the bound eigenfunctions, these couplings were calculated with a constant dipole of 9.9 debye [43]. A given vibrational level of the ground state has several nonvanishing dipole couplings with vibrational levels of the excited state. Figure 2 along with Fig. 3 reveals several possible intermediate and final levels for the pathway 1. Similar to Fig. 2, Fig. 4 shows the absolute value of the transition dipole moment $|\langle\phi_v|\mu_{ge}|\phi_n\rangle|$ from the unbound level to the bound levels v of the ground electronic state. This figure evidences the possible transitions regarding the second photoassociation pathway. The couplings are larger in the far infrared and, in particular, the maximum photoassociation

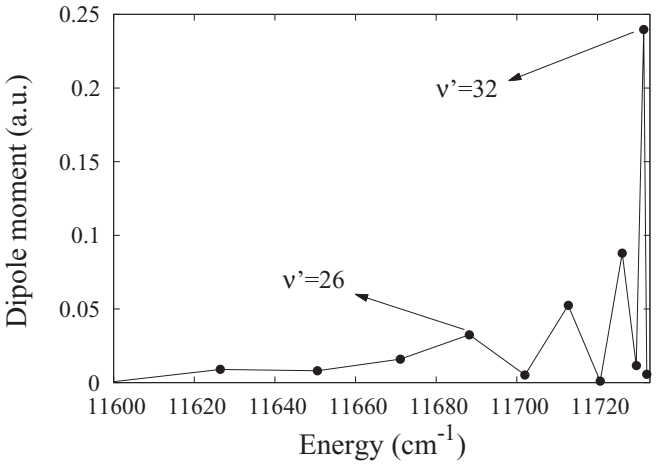

FIG. 2. Dipole moment of LiCs for transitions from a free level with energy 0.035 cm^{-1} of the $X\,^1\Sigma$ state to the bound vibrational levels of the $B\,^1\Pi$ state as a function of the corresponding transition energy.

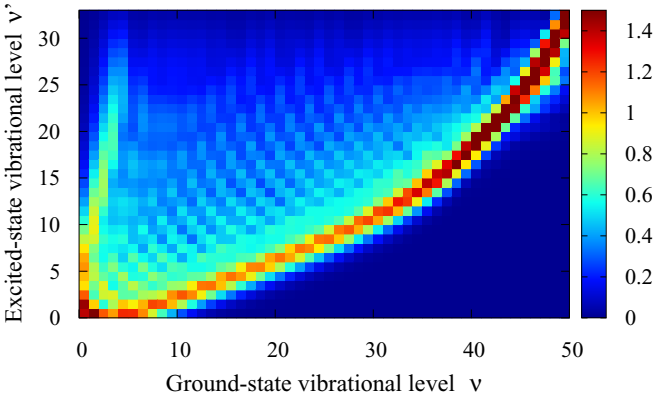

FIG. 3. Dipole moment between the bound vibrational levels of the $X\,^1\Sigma$ and $B\,^1\Pi$ states of LiCs.

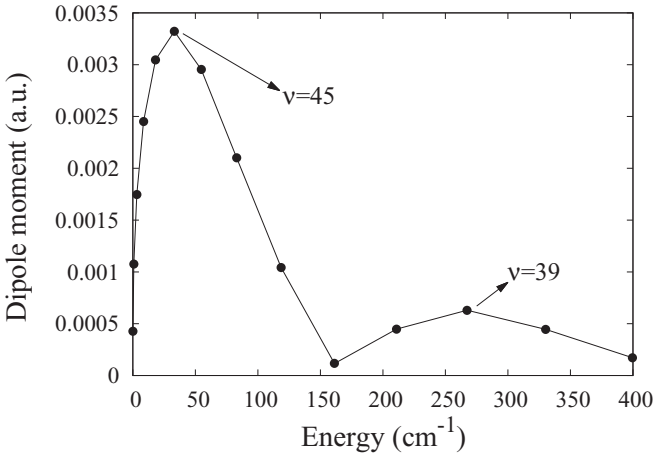

FIG. 4. Dipole moment of LiCs for transitions from a free level with energy 0.035 cm^{-1} to the bound vibrational levels within the $X\,^1\Sigma$ state as a function of the corresponding transition energy.

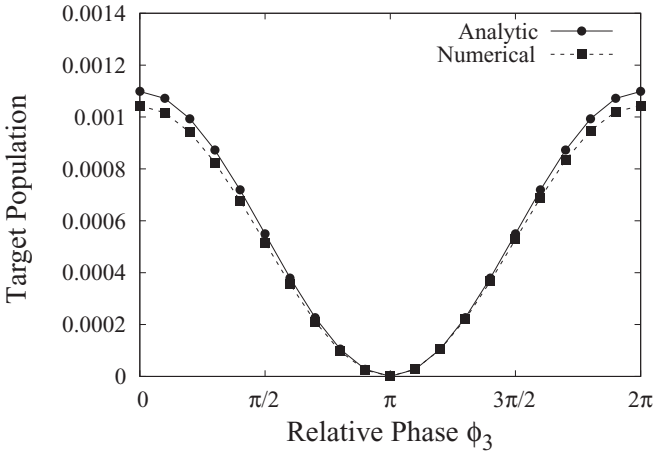

FIG. 5. Population of the target state $\nu = 45$ as a function of the phase ϕ_3. Comparison of the analytic result of Eq. (14) with direct numerical calculations.

dipole moment occurs for the vibrational level $\nu = 45$ corresponding to a transition frequency of approximately 33 cm^{-1}.

III. COHERENT CONTROL

We illustrate the photoassociation scheme choosing the $\nu = 45$ bound vibrational level of the ground state as our target state. As seen in the previous section, this level has a strong coupling with the initial unbound levels of the ground state, being a convenient choice for the second pathway. Regarding the first pathway, we choose the $\nu' = 32$ bound vibrational level of the excited state as the intermediate state also due to its strong coupling with the initial unbound levels. We stress that other choices for the intermediate and target levels are possible, while not qualitatively changing our conclusions.

In order to numerically solve the time-dependent Schrödinger equation, we have expanded the wave function in the basis of the energy eigenfunctions, truncating the number of discretized continuum levels for each electronic state. Substituting the expansion in Eq. (4) yields a coupled system of first-order differential equations for the expansion coefficients. The corresponding unitary propagator $U(t,0)$ is then written in terms of a series of short-time step propagators $U(t+\Delta t,t)$ and each short-time propagator is in turn approximated by a second-order split operator, leading to the evolution of the wave function $|\psi(t+\Delta t)\rangle = U(t+\Delta t,t)|\psi(t)\rangle$ (for details, see Refs. [28,44]).

Figure 5 compares the results of the perturbative approach expressed in Eq. (14) with the direct numerical calculations for the total transition probability to the target level as a function of the phase ϕ_3. The initial state is chosen to be a scattering level of the ground electronic state corresponding to $E_n \approx 50$ mK. The phases ϕ_1 and ϕ_2 are set to zero and the pulse frequencies are set to the corresponding resonance frequencies. The amplitudes of the pulses are $\varepsilon_1 = 0.1$ kV cm^{-1}, $\varepsilon_2 = 0.25$ kV cm^{-1}, and $\varepsilon_3 = 0.46$ kV cm^{-1}, while the pulse widths are $\tau_1 = 1000$ ps, $\tau_2 = 1000$ ps, and $\tau_3 = 2000$ ps. We observe that the perturbation theory is able to capture the role of the phase of the third pulse in controlling the transition probability.

In order to verify the control scheme out of the perturbative regime, we have performed numerical calculations taking the initial wave function representing the atomic collision as a Gaussian wave packet in the electronic ground state,

$$\langle r|\psi(t=0)\rangle = \begin{pmatrix} \left(\frac{2}{\pi a^2}\right)^{1/4} \exp\left[i\kappa r - \frac{(r-r_0)^2}{a^2}\right] \\ 0 \end{pmatrix}, \qquad (16)$$

where a and r_0 define respectively the initial width and the central position of the wave packet, while $\kappa < 0$ sets the initial collision momentum. For the time propagation, we have considered an initial state with position $r_0 = 450$ a.u., width $a = 100$ a.u., and with collision energy corresponding to 50 mK. This wave packet is placed far from the interaction region, i.e., at $t = 0$ the potentials and dipole functions are negligible over the wave-packet range.

Figure 6 shows the vibrational population dynamics taking into account only the first pathway by setting $\varepsilon_3 = 0$. The amplitudes and frequencies of the pulses are $\varepsilon_1 = 1.1$ kV cm^{-1}, $\varepsilon_2 = 18.35$ kV cm^{-1}, $\omega_1 = 11\,731$ cm^{-1}, and $\omega_2 = 11\,764$ cm^{-1}, with no phase difference $\phi_1 = \phi_2 = 0$. The frequency ω_1 is just the corresponding transition energy from the initial state to the $\nu' = 32$ level, while ω_2 corresponds to the energy gap between this level and the target level. The durations of the pulses are $\tau_1 = 400$ ps and $\tau_2 = 500$ ps and the central times $t_1' = 1260$ ps and $t_2' = 2300$ ps. For these choices, the final population of the target level, which essentially equals the overall bound population of the ground state, reaches approximately 0.17 and the population of the electronic bound levels reaches approximately 0.24. As usual in pump-dump processes, some degree of control over the final populations results from either manipulating the timing or the relative phase of the pulses. However, for the above amplitudes and frequencies, no appreciable increase of the final population of the target level is observed manipulating either t_2' or ϕ_2.

Figure 7 shows the vibrational population dynamics related to the second pathway only, by setting $\varepsilon_1 = 0$ and $\varepsilon_2 = 0$. The amplitude and frequency of the pulse are $\varepsilon_3 = 51.13$ kV cm^{-1} and $\omega_3 = 33.19$ cm^{-1} with $\phi_3 = 0$. The duration of the pulse is $\tau_3 = 585$ ps and its central time is $t_3' = 1900$ ps. For

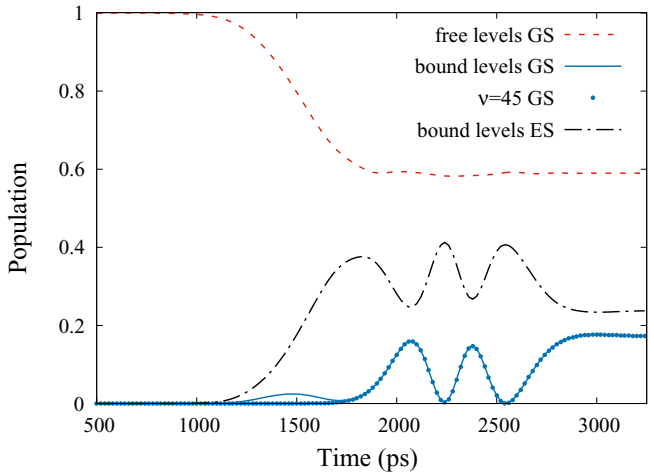

FIG. 6. Population dynamics induced by a pair of pump-dump pulses according to the photoassociation pathway 1. Population of the unbound levels of the electronic ground state (GS) (red dashed curve), population of the bound levels of the ground state (blue solid curve), population of the $v = 45$ ground vibrational level (blue points), and population of the bound levels of the electronic excited state (ES) (black dotted-dashed curve).

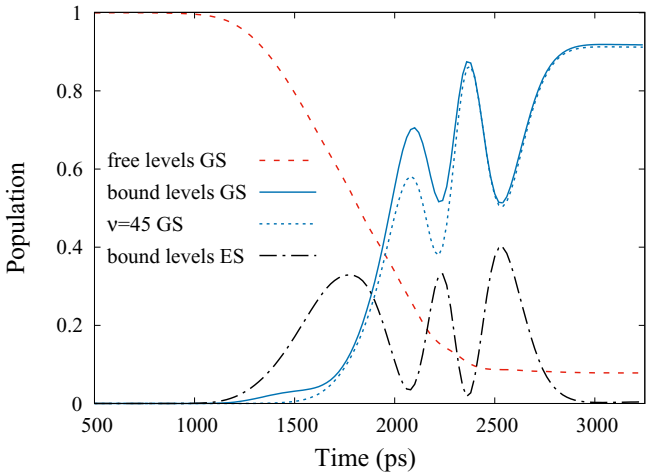

FIG. 8. Population dynamics induced by three pulses combining the photoassociation pathways 1 and 2. Population of the unbound levels of the electronic ground state (GS) (red dashed curve), population of the bound levels of the ground state (blue solid curve), population of the $v = 45$ ground vibrational level (blue short-dashed curve), and population of the bound levels of the electronic excited state (ES) (black dotted-dashed curve).

this pathway, no appreciable population is observed in the electronic excited state. Apart from times around $t = 2000$ ps, the overall bound population of the ground state remains in the target level. The final population reached by the target level is 0.52.

Figure 8 shows the combined effects of the three pulses ($\varepsilon_i \neq 0$), with the same pulse parameters given above. The population of the target level reaches approximately 0.92 at the final time, which essentially equals the final overall bound population of the ground state. There are some oscillations between the populations of the ground and the excited states between $t = 1500$ ps and $t = 3000$ ps, as also observed in Fig. 6, but now these oscillations result in a more effective transfer of the population to the ground state. The possibility of coherent control of the vibrational population of the target level by the interference of the two pathways is shown in Fig. 9, where the final bound population of the ground state is presented as a function of the phase ϕ_3 and timing of pulse 3 $t_3' - t_1'$ relative to the pulse 1. The target population can vary from a negligible value up to 0.92 with the manipulation of these parameters. The maximum value is observed for the pulse 3 in between the pump and dump pair, $t_3' - t_1' = 640$ ps, when the target population is beginning to be populated through pathway 1.

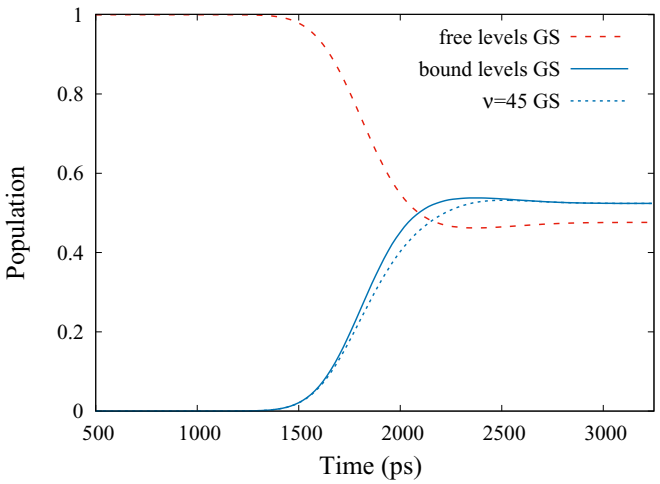

FIG. 7. Population dynamics induced by a single far-IR pulse according to the photoassociation pathway 2. Population of the unbound levels of the electronic ground state (GS) (red dashed curve), population of the bound levels of the ground state (blue solid curve), and population of the $v = 45$ ground vibrational level (blue short-dashed curve).

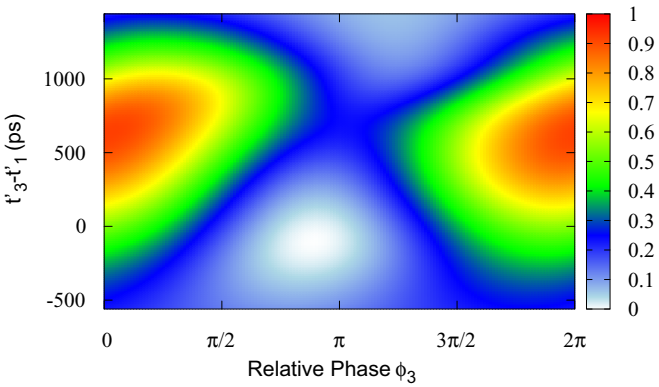

FIG. 9. Final bound population of the ground electronic state combining the photoassociation pathways 1 and 2 as a function of the phase ϕ_3 and the timing $t_3' - t_1'$ of pulse 3 relative to pulse 1.

IV. CONCLUSIONS

The paper presents a scheme for the formation of cold heteronuclear molecules in bound levels of the electronic ground state by means of the combination of two photoassociation pathways involving near-IR pump-dump pulses and a far-IR pulse. A perturbative analysis and direct numerical calculations show that the relative phase and timing of the pulses can be used as convenient control knobs for the formation of such molecules due to the interference of these two pathways. Though the formation of cold molecules has been the main focus here, the same ideas may also be adapted for photoassociation in the thermal regime, with suitable choices for the durations of the pulses and appropriate description of the initial thermal distribution [45,46]. In practice, the ground vibrational levels that are reachable through this technique are those with a nonzero electric dipole coupling with the initial free state, usually vibrational levels with intermediate to high values of the vibrational quantum number. In order to produce vibrationally cold molecules, a subsequent vibrational stabilization step needs to be performed. This step can be accomplished, for instance, applying an additional chirped pulse or a fully optimized pulse [47–50]. Furthermore, thanks to the existence of an associated permanent dipole in heteronuclear molecules, this stabilization process can be carried out within the ground electronic state with IR radiation [44]. Finally, it is worth mentioning that the technology for generating pulses in the far-IR frequency domain (also known as the therahertz range) is becoming available in the laboratory [51].

ACKNOWLEDGMENTS

The author acknowledges support from Sao Paulo Research Foundation, FAPESP (Grant No. 2014/23648-9) and from National Council for Scientific and Technological Development, CNPq (Grant No. 473283/2013-1).

[1] J. L. Carini, S. Kallush, R. Kosloff, and P. L. Gould, J. Phys. Chem. A **120**, 3032 (2016).
[2] G. Quéméner and P. S. Julienne, Chem. Rev. **112**, 4949 (2012).
[3] M. T. Bell and T. P. Softley, Mol. Phys. **107**, 99 (2009).
[4] L. D. Carr, D. DeMille, R. V. Krems, and J. Ye, New J. Phys. **11**, 055049 (2009).
[5] M. Guo, B. Zhu, B. Lu, X. Ye, F. Wang, R. Vexiau, N. Bouloufa-Maafa, G. Quéméner, O. Dulieu, and D. Wang, Phys. Rev. Lett. **116**, 205303 (2016).
[6] P. K. Molony, P. D. Gregory, Z. Ji, B. Lu, M. P. Köppinger, C. R. Le Sueur, C. L. Blackley, J. M. Hutson, and S. L. Cornish, Phys. Rev. Lett. **113**, 255301 (2014).
[7] T. Takekoshi, L. Reichsöllner, A. Schindewolf, J. M. Hutson, C. R. Le Sueur, O. Dulieu, F. Ferlaino, R. Grimm, and H.-C. Nägerl, Phys. Rev. Lett. **113**, 205301 (2014).
[8] J. Deiglmayr, A. Grochola, M. Repp, K. Mörtlbauer, C. Glück, J. Lange, O. Dulieu, R. Wester, and M. Weidemüller, Phys. Rev. Lett. **101**, 133004 (2008).
[9] S. Ospelkaus, A. Peér, K.-K. Ni, J. J. Zirbel, B. Neyenhuis, S. Kotochigova, P. S. Julienne, J. Ye, and D. S. Jin, Nat. Phys. **4**, 622 (2008).
[10] C. R. Menegatti, B. S. Marangoni, and L. G. Marcassa, Laser Phys. **18**, 1305 (2008).
[11] J. M. Sage, S. Sainis, T. Bergeman, and D. DeMille, Phys. Rev. Lett. **94**, 203001 (2005).
[12] A. J. Kerman, J. M. Sage, S. Sainis, T. Bergeman, and D. DeMille, Phys. Rev. Lett. **92**, 033004 (2004).
[13] A. V. Avdeenkov and J. L. Bohn, Phys. Rev. Lett. **90**, 043006 (2003).
[14] J. L. Carini, S. Kallush, R. Kosloff, and P. L. Gould, Phys. Rev. Lett. **115**, 173003 (2015).
[15] K. Aikawa, D. Akamatsu, M. Hayashi, K. Oasa, J. Kobayashi, P. Naidon, T. Kishimoto, M. Ueda, and S. Inouye, Phys. Rev. Lett. **105**, 203001 (2010).
[16] J. Ulmanis, J. Deiglmayr, M. Repp, R. Wester, and M. Weidemller, Chem. Rev. **112**, 4890 (2012).
[17] A. Homer and G. Roberts, Phys. Rev. A **78**, 053404 (2008).
[18] K. M. Jones, E. Tiesinga, P. D. Lett, and P. S. Julienne, Rev. Mod. Phys. **78**, 483 (2006).
[19] B.-B. Wang, Y.-C. Han, and S.-L. Cong, J. Chem. Phys. **143**, 094303 (2015).
[20] U. Poschinger, W. Salzmann, R. Wester, M. Weidemüller, C. P. Koch, and R. Kosloff, J. Phys. B **39**, S1001 (2006).
[21] C. P. Koch and R. Moszyński, Phys. Rev. A **78**, 043417 (2008).
[22] C. P. Koch, E. Luc-Koenig, and F. Masnou-Seeuws, Phys. Rev. A **73**, 033408 (2006).
[23] C. P. Koch and M. Shapiro, Chem. Rev. **112**, 4928 (2012).
[24] C. Brif, R. Chakrabarti, and H. Rabitz, New J. Phys. **12**, 075008 (2010).
[25] P. Brumer and M. Shapiro, Chem. Phys. Lett. **126**, 541 (1986).
[26] D. J. Tannor and S. A. Rice, J. Chem. Phys. **83**, 5013 (1985).
[27] D. J. Tannor, R. Kosloff, and S. A. Rice, J. Chem. Phys. **85**, 5805 (1986).
[28] E. F. de Lima, J. Low Temp. Phys. **180**, 161 (2015).
[29] S. Kotochigova, Phys. Rev. Lett. **99**, 073003 (2007).
[30] Y.-Y. Niu, S.-M. Wang, and S.-L. Cong, Chem. Phys. Lett. **428**, 7 (2006).
[31] E. F. de Lima and J. E. Hornos, Chem. Phys. Lett. **433**, 48 (2006).
[32] M. Korolkov, J. Manz, G. Paramonov, and B. Schmidt, Chem. Phys. Lett. **260**, 604 (1996).
[33] E. F. de Lima, T.-S. Ho, and H. Rabitz, J. Phys. A: Math Theor. **41**, 335303 (2008).
[34] C. Cohen-Tannoudji, J. Dupont-Roc, and G. Grinberg, *Atom-Photon Interactions* (John Wiley & Sons Inc., New York, 1992).
[35] N. Dudovich, B. Dayan, S. M. Gallagher Faeder, and Y. Silberberg, Phys. Rev. Lett. **86**, 47 (2001).
[36] D. A. Fedorov, A. Derevianko, and S. A. Varganov, J. Chem. Phys. **140**, 184315 (2014).
[37] N. Mabrouk, H. Berriche, H. B. Ouada, and F. X. Gadea, J. Phys. Chem. A **114**, 6657 (2010).
[38] A. Grochola, A. Pashov, J. Deiglmayr, M. Repp, E. Tiemann, R. Wester, and M. Weidemüller, J. Chem. Phys. **131**, 054304 (2009).

[39] P. Staanum, A. Pashov, H. Knöckel, and E. Tiemann, Phys. Rev. A **75**, 042513 (2007).
[40] M. Aymar and O. Dulieu, J. Chem. Phys. **122**, 204302 (2005).
[41] A. Derevianko, E. Luc-Koenig, and F. Masnou-Seeuws, Can. J. Phys. **87**, 67 (2009).
[42] H. Bachau, E. Cormier, P. Decleva, J. E. Hansen, and F. Martn, Rep. Prog. Phys. **64**, 1815 (2001).
[43] J. Deiglmayr, M. Repp, A. Grochola, K. Mortlbauer, C. Gluck, O. Dulieu, J. Lange, R. Wester, and M. Weidemuller, Faraday Discuss. **142**, 335 (2009).
[44] E. F. de Lima, T.-S. Ho, and H. Rabitz, Chem. Phys. Lett. **501**, 267 (2011).
[45] E. F. de Lima, T.-S. Ho, and H. Rabitz, Phys. Rev. A **78**, 063417 (2008).
[46] L. Levin, W. Skomorowski, L. Rybak, R. Kosloff, C. P. Koch, and Z. Amitay, Phys. Rev. Lett. **114**, 233003 (2015).
[47] D. M. Reich and C. P. Koch, New J. Phys. **15**, 125028 (2013).
[48] E. F. de Lima, T.-S. Ho, and H. Rabitz, Phys. Rev. A **89**, 043421 (2014).
[49] M. Ndong and C. P. Koch, Phys. Rev. A **82**, 043437 (2010).
[50] C. P. Koch, J. P. Palao, R. Kosloff, and F. Masnou-Seeuws, Phys. Rev. A **70**, 013402 (2004).
[51] M. C. Hoffmann and J. A. Flp, J. Phys. D: Appl. Phys. **44**, 083001 (2011).